

## MICROFABRICATION OF VERTICAL CAVITY SURFACE EMITTING LASER CAVITIES

A. Scherer, J.L. Jewell\*, J.P. Harbison<sup>+</sup>, K. Uomi<sup>+</sup>,  
B.J. Yoo<sup>+</sup>, R.J. Bhat<sup>+</sup>, M. Walther<sup>+</sup>

California Institute of Technology, Pasadena, CA 91125

\*Photonics Research Inc. Longmont, CO 80503

<sup>+</sup>Bellcore, Red Bank, NJ 07701

### ABSTRACT

We have reduced the threshold voltages and currents of vertical cavity surface emitting lasers by using dielectric high reflectivity mirrors which were deposited after the diode fabrication step. This device fabrication sequence is able to correct for inaccuracies in the crystal growth and allows the future development of more complex laser structures. The quantum-well based laser diodes were demonstrated at 0.72 $\mu\text{m}$ , 0.85 $\mu\text{m}$ , and 1.55 $\mu\text{m}$ . Threshold currents and voltages of our 0.85  $\mu\text{m}$  lasers were 2.8 mA at 1.7 V pulsed, and 4 mA when cw-pumped. The threshold currents of 5x7  $\mu\text{m}^2$  area 1.55  $\mu\text{m}$  devices were 17 mA.

### INTRODUCTION

Low threshold vertical cavity surface emitting lasers (VCSELs) have become very interesting devices as a result of their ability to be integrated into large two-dimensional arrays. Electrically pumped VCSELs have been reported with emission wavelengths ranging from 630nm to 1.55 $\mu\text{m}$  [1-8]. These versatile devices are expected to find uses in multi-head memory, laser printing, metrology, 2D scanning, visual displays, fiber communications, optical interconnects, and optical computing. We have developed and demonstrated a new laser structures which have achieved low threshold voltage and currents and improved power dissipation and wall plug efficiency. This was accomplished by removing the highly resistive p-doped mirror/contact from the electric pumping path, and using high-reflectivity sputter-deposited dielectric mirrors [9]. Laser diodes were fabricated with emission wavelengths ranging from the visible (720 nm) to the IR (1.55  $\mu\text{m}$ ) by using such dielectric mirrors.

The VCSEL designs consist of epitaxially grown p-i-n junctions with quantum well active regions, as well as grown n- and p-doped cladding layers. The optical laser cavities were formed by high-reflectivity dielectric mirror deposition at least on the p-doped side of the

laser cavity. For MBE-grown samples, n-doped epitaxial mirror/contact layers were used, and a hybrid semiconductor/dielectric mirror design was developed. This new electrical pumping geometry has allowed us to fabricate lasers with threshold voltages as low as 1.7 V for GaAs VCSELs, and offers several important advantages over the more conventional all-epitaxial laser designs: Since the optical cavity is accessible to precise tuning of its length as well as to microfabrication before the deposition of the dielectric mirror layers, this device structure is ideally suited for control over the polarization, the near- and far-field patterns of discrete devices, as well as the fabrication of variable wavelength laser diode arrays.

## PROCEDURE

### 850 nm GaAs quantum well lasers

The schematic diagram of GaAs quantum well lasers is shown in Figure 1. Light at 850 nm is generated by the 10 nm GaAs quantum wells and is emitted through the annular p-contact. The p-side resistance is reduced by heavily doping the 1  $\mu\text{m}$  spacer at the top of the cavity, and completely avoiding the well/barriers inherent in epitaxially grown mirror-contact structures. This requires a high reflectivity molecular beam epitaxially (MBE) grown n-doped bottom mirror, which is matched to the laser emission wavelength, as well as a good dielectric top mirror.

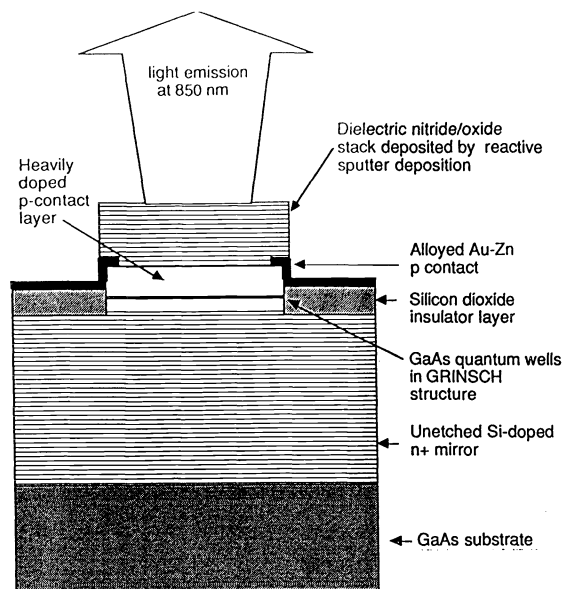


Figure 1. Schematic of the low-voltage VCSEL operating at 850 nm.

Molecular beam epitaxy was used to grow 30 pairs of n-doped  $\text{Al}_{0.15}\text{Ga}_{0.85}\text{Al}/\text{AlAs}$  bottom mirror layers, the active p-n junction containing three 10 nm GaAs quantum wells

separated by 12 nm  $\text{Al}_{0.3}\text{Ga}_{0.7}\text{As}$  layers and a 1  $\mu\text{m}$  p-doped top contact. 12 pairs of alternating  $\text{SiO}_2/\text{Si}_3\text{N}_4$  layers formed a high-reflectivity mirror which completed the laser cavity. We have evaluated these reactive sputter deposited mirrors using finesse measurements in resonator structures, and obtain reflectivities of 98.3% in 9.5 pairs [10]. Individual laser elements were defined by ion etching of mesas through the pn junction, followed by deposition of  $\text{SiO}_2$  to define the current path. Au-Zn p-contacts were then deposited around the mesa tops and alloyed for current injection (Figure 2). Finally, another ion milling step was used to isolate individual contacts. The fabrication sequence is summarized in Figure 2. Lasers with diameters ranging from 7.5  $\mu\text{m}$  to 25  $\mu\text{m}$  were thus fabricated and measured.

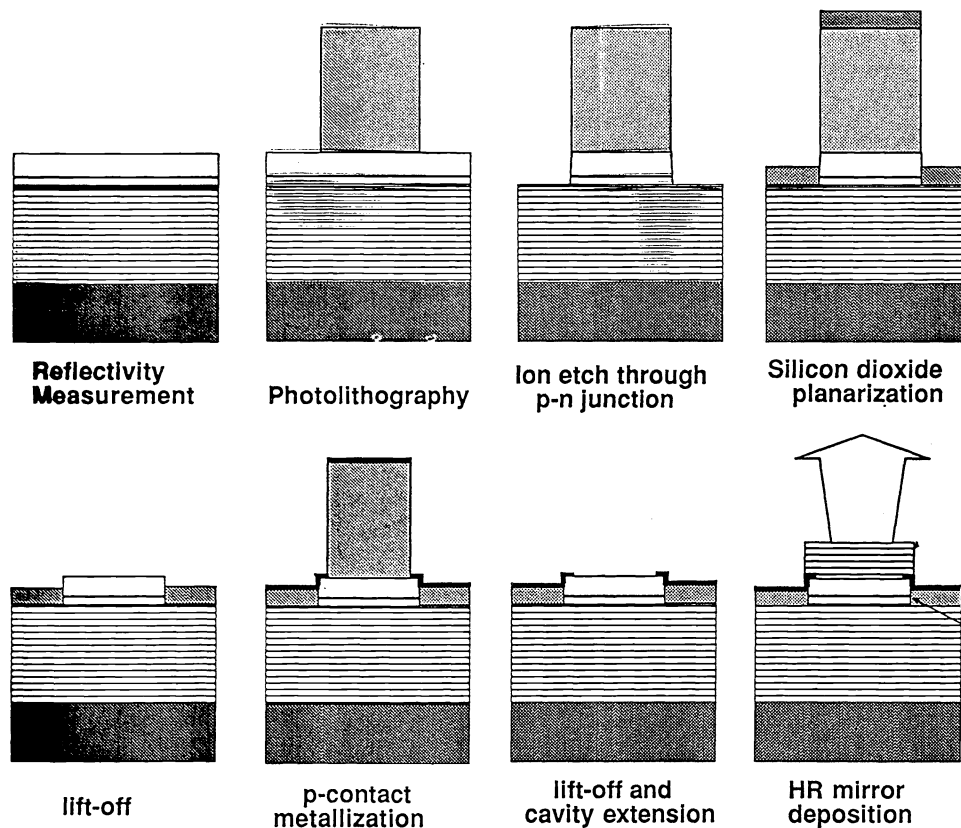


Figure 2. Processing sequence for fabrication of the low-voltage 850 nm VCSEL.

The visible 720nm AlAs/GaAs laser design, is very similar to the GaAs quantum well laser design. In this device, light is emitted from a GaAs/AlAs superlattice, and again emits

through an annular top AuZn metal contact. Since the top epilayer contact has a high aluminum concentration to avoid reabsorption of the emitted light, these laser diodes require additional steps during the fabrication procedure. Molecular beam epitaxy was used to deposit 33 pairs of n-doped  $\text{Al}_{0.3}\text{Ga}_{0.7}\text{As}/\text{AlAs}$  mirror layers, followed by an active region consisting of  $0.57\text{nm AlAs}/2.26\text{nm GaAs}$  superlattice with an average Al concentration of about 0.3. A  $0.88\text{ }\mu\text{m}$  thick p-doped top contact was then deposited on top of this diode structure. After the fabrication of discrete diodes, the cavity was completed by deposition of twelve  $\text{SiO}_2/\text{Si}_3\text{N}_4$  dielectric Bragg reflector pairs which were deposited by rf-magnetron sputtering [10]. We used the same processing sequence described in Figure 1a to define the individual laser diode elements. However, to protect the surface from oxidation and etching during processing, a thin GaAs cap layer was deposited during MBE growth. This layer was removed by ion milling in an additional step just before the deposition of the dielectric reflector.

### 1.55 $\mu\text{m}$ InGaAsP/InP lasers

The laser design for this wavelength is shown in Figure 3, and required somewhat more intricate processing. To obtain a good optical cavity in which the active material matched the luminescence wavelength, we decided to use broad-band dielectric mirrors on both sides of the laser cavity. Since a short cavity is desired for reducing diffraction-related losses, the fabrication of these lasers involved the local removal of the substrate underneath the laser elements. Furthermore, a "mushroom"-type p-contact defined by selective chemical etching of the active material was used for more efficient electrical pumping underneath the high reflectivity mirror layers.

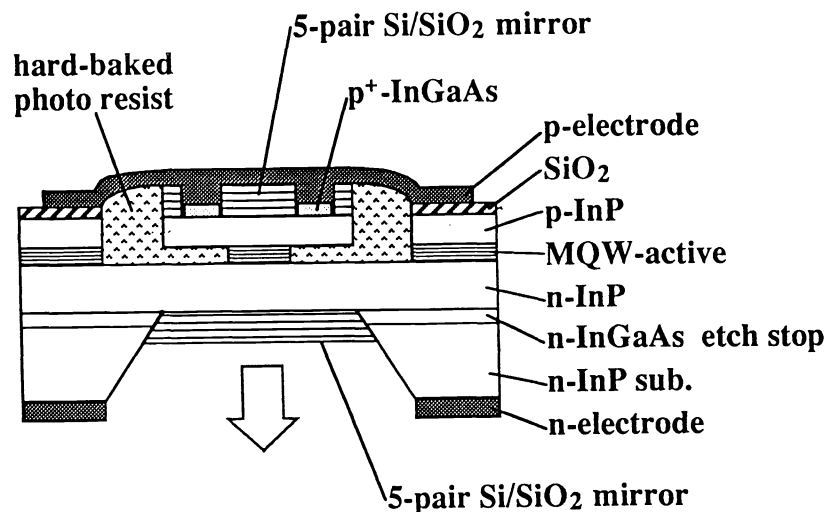


Figure 3. Schematic cross-section of the  $1.55\text{ }\mu\text{m}$  VCSEL.

Organometallic vapor phase epitaxy (OMVPE) was used to grow multiple quantum well active material for the VCSELs on an n-type (001) InP substrate. The grown layer consisted of a  $0.2\text{ }\mu\text{m}$  n-InGaAs etch-stop layer, a  $0.65\text{ }\mu\text{m}$  n-InP cladding layer, an unstrained multiple quantum well active layer, a  $0.89\text{ }\mu\text{m}$  p-InP cladding layer and a  $0.2\text{ }\mu\text{m}$

p-InGaAs cap layer. The active layer was theoretically optimized to be composed of twelve 7 nm InGaAs wells separated by 6 nm thick InGaAsP barriers, to form a total active material thickness of about  $3/4n\lambda$ . This layer was located at the peak of the optical standing wave to achieve matched gain.

First, a 5-pair mirror stack of Si/SiO<sub>2</sub> was deposited through a photolithographically defined mask and lifted off. This mask shape was then transferred by chemical mesa etching through the p-doped InP surface layer, through the quantum well region, and into the n-type bottom contact epilayer. Then, a selective chemical etch of only the quantum well active material was used to obtain the final active volumes of 5x7 and 7x10  $\mu\text{m}^2$  underneath the high reflectivity mirror. The diamond shaped active layer was automatically formed by the larger etching rate in the [010] direction than that in both [011] and [01-1] directions. The VCSEL was then embedded in hard-baked photoresist and the p-contact metal was deposited on top of the mesa. Following the preparation of the wafer surface, windows were etched through the InP substrate by a chemical etch which stopped at the InGaAs layer. We thereby defined 2  $\mu\text{m}$  thin membranes underneath each laser diode. These membranes were then coated with a second high-reflectivity mirror to generate a high-finesse optical cavity with a cavity length of  $9x\lambda/2n$ . Figure 4 shows the fabrication sequence used for these lasers.

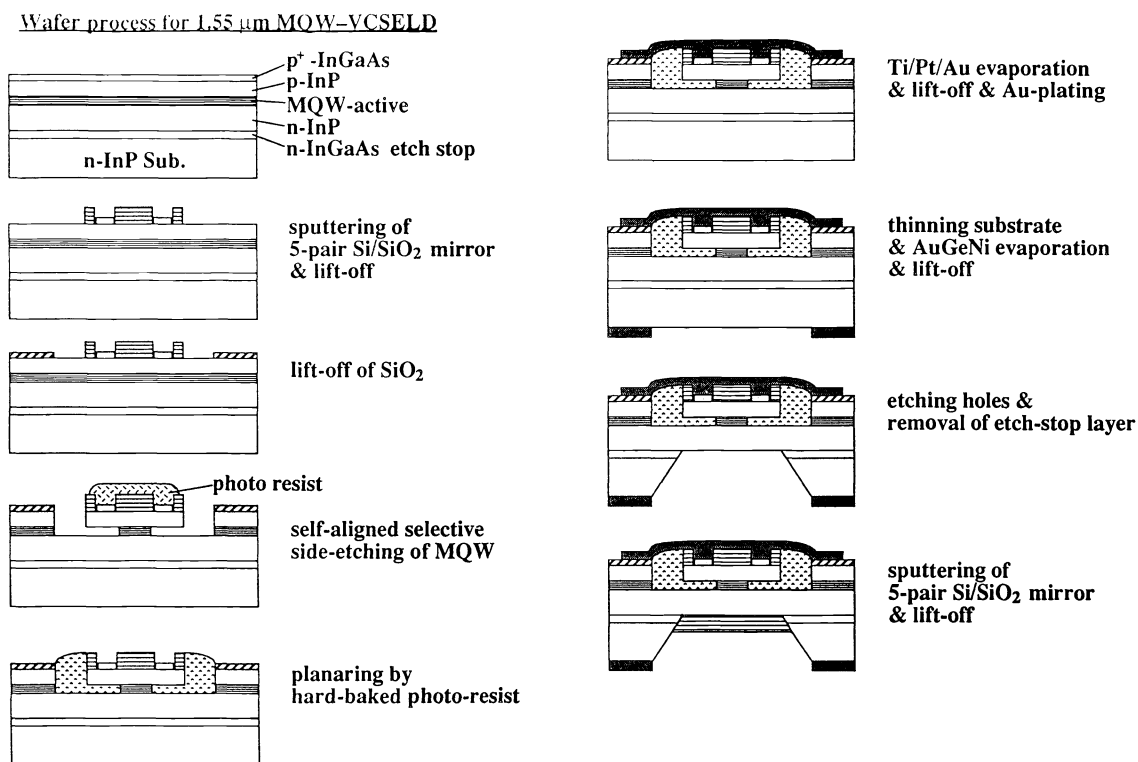


Figure 4. Processing sequence used for fabrication of the 1.55  $\mu\text{m}$  VCSEL.

## RESULTS AND DISCUSSION

### GaAs/AlAs lasers

The p-side resistance is reduced by heavily beryllium-doping the top of the cavity and completely avoiding the barriers inherent in epitaxially grown mirror/contact structures. The current-voltage characteristics of this configuration show a reduced series resistance of 67 ohms for 12  $\mu\text{m}$  lasers, averaged between the bandgap voltage (1.4 V) and the 2.0 V operating voltage. In contrast to the parabolic profile of most VCSEL current-voltage (I-V) plots, this IV characteristic is fairly linear right from the bandgap value. Resulting resistance  $\times$  area products are less than  $7 \times 10^{-5} \Omega \cdot \text{cm}^2$ , nearly as low as the  $5 \times 10^{-5} \Omega \cdot \text{cm}^2$  calculated for high-power single-mode edge-emitting lasers. Figure 5a shows the light-current characteristics with a threshold current of 2.8 mA under pulsed operation. At DC current, this value increases to 4 mA due to poor heat sinking. Figure 5b shows two spectra of 12  $\mu\text{m}$  diameter lasers. The spontaneous emission of the 10 nm thick quantum wells below threshold is shown in the lower part of Figure 5b, and is centered around 850 nm. Above threshold the laser emits single mode at 855 nm wavelength.

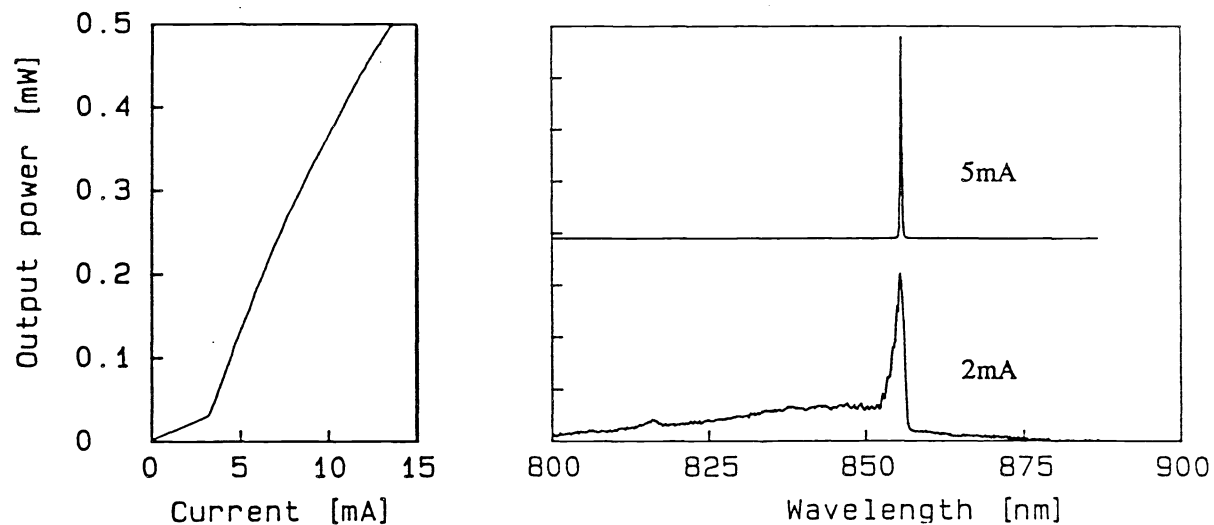


Figure 5 (a) L-I curve from 12  $\mu\text{m}$  diameter VCSEL pulsed with 1% duty cycle and (b) output spectra at 2 mA (below threshold) and 5 mA (above threshold).

A great advantage of this hybrid laser design over previous monolithic laser structures lies in the relaxation of accuracy required during crystal growth. Thus, even if the cavity length is not tuned correctly to the quantum well emission wavelength, and the bottom mirror reflectivity maximum, the top dielectric mirror stack can be redesigned to compensate for such growth inaccuracy. This kind of re-tuning was required with this

particular wafer. Figure 6a shows the measured reflectivity spectrum for the grown wafer, and it is evident that the measured cavity resonance peaks at 826 nm and 882 nm are far from the designated wavelength of 850 nm. This places the resonance as far from the optimum wavelength as possible. However, we can still fabricate lasers from this structure by compensating the cavity length discrepancy with a  $1/4$  wavelength of  $\text{Si}_3\text{N}_4$  cavity extension layer before depositing the dielectric top mirror. Figure 6b shows the resulting spectrum including the correction layer and the  $\text{SiO}/\text{Si}_3\text{N}_4$  top mirror and the resonance is indeed shifted close to 850 nm. Although in principle this adjustment should severely compromise the laser performance since the  $\text{GaAs}/\text{Si}_3\text{N}_4$  interface actually reduces the reflectivity of the mirror stack, the desirable device characteristics mentioned above are still obtained. This demonstrates the power of being able to deposit the upper portion of the Fabry-Perot cavity during processing to allow corrections of slight changes in layer thicknesses.

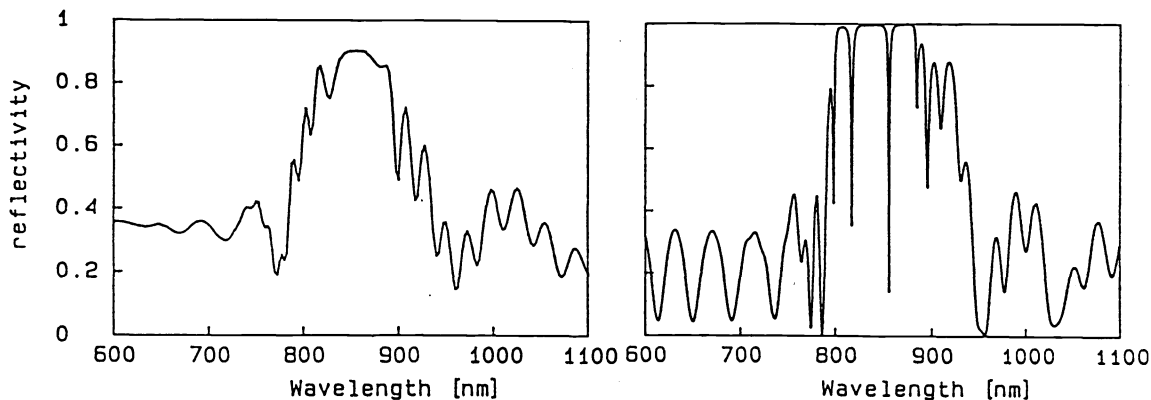


Figure 6 (a) measured R vs wavelength from grown wafer and (b) corrected spectrum with correction of the spacer by introducing a  $\text{Si}_3\text{N}_4$  correction layer and top mirrors.

Smaller changes in the effective cavity length are obtained by controlling the top dielectric mirror thickness and we have tuned the emission wavelength from 850 to 855 nm. Further change of the wavelength is possible at the expense of higher threshold currents. This laser design also lends itself to microfabrication of focusing or polarizing optics in or close to the cavity. Sputter-deposition of the passive dielectric mirrors does not require the clean, contamination-free surfaces and high growth temperatures necessary for epitaxial growth, and thus can be performed at the end of the fabrication procedure, allowing for on wafer testing and correction using optical analysis. Emission at much shorter wavelengths is possible by changing the active material from GaAs to AlGaAs, as we have demonstrated in the superlattice VCSEL operating at 720 nm. In the resulting visible lasers, we have

observed threshold currents of 40 mA for 20  $\mu\text{m}$  diameter devices, which we expect to reduce further. In this design, the cavity length was again adjusted for optimum match with the emission wavelength. Still shorter wavelengths are expected to be obtained with InGaP/InGaAlP active material, and preliminary results show that highly efficient diodes can be produced with low surface recombination rates.

### InGaAs/InP lasers

Figure 7a shows the emission spectrum of a  $5 \times 7 \mu\text{m}^2$  device under 2 mA cw pumping at room temperature. Two longitudinal modes with mode spacing (FSR) of 165 nm was clearly observed. The value of the free spectral range is in good agreement with the calculated one using device parameters. The finesse value evaluated from FSR and spectral width (0.7 nm) is about 240, which corresponds to one round-trip  $R_{\text{total}}$  of 98.7%. The difference between  $R$  and  $R_{\text{total}}$  was 0.5 %, which resulted from the diffraction loss in the cladding layers and the scattering loss in the active layer. The device resistances were  $130 \Omega$  and  $90 \Omega$  for  $5 \times 7$  and  $7 \times 10 \mu\text{m}^2$  devices, respectively. Figure 8a shows the light output versus current characteristics for these 1.5  $\mu\text{m}$  VCSELs. The light output versus current curve for a  $5 \mu\text{m}$  device is shown in Figure 8b, and we obtain a pulsed threshold current of approximately 17 mA. The threshold current density  $J_{\text{th}}$  was estimated to be 50 and 35  $\text{kA}/\text{cm}^2$  for  $5 \times 7 \mu\text{m}^2$  and  $7 \times 10 \mu\text{m}^2$  devices, respectively, which was about 5 times higher than the theoretically predicted value. This discrepancy may be caused by non uniform current injection into the active layer which results from the lateral diffusion in both the p and n cladding layer [11].

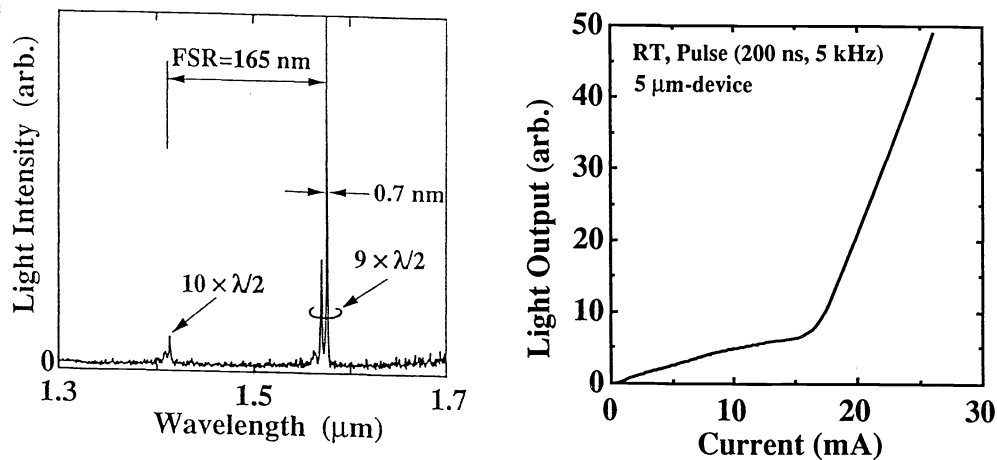


Figure 7 (a) emission spectrum of a 1.55  $\mu\text{m}$  VCSEL under 2 mA cw pumping. (b) L-I curve of a  $5 \times 7 \mu\text{m}^2$  laser.



## CONCLUSIONS

We have identified some important advantages of using dielectric mirrors as part of the laser cavity. The most important improvements over the all-epitaxial vertical cavity laser design are discussed below: First, the resistance of the laser is reduced by the elimination of the p-mirror as top contact. This improvement in electrical conductivity results in lower thermal dissipation, and thereby allows a higher packing density of laser elements into arrays. It is also easier to obtain continuous wave laser operation and a higher wallplug efficiency from low-voltage laser diodes. Secondly, the growth requirements are significantly simplified and tolerances relaxed, so that it is easier to grow these structures with a minimum of calibration. In fact, we show that the laser cavity can be adjusted at the end of the fabrication step by the introduction of an appropriate spacer layer. This flexibility is especially useful for phosphide-containing lasers, which are generally grown by organo-metallic vapor phase epitaxy (OMVPE), since in this technique the absolute layer thickness is more difficult to control than in molecular beam epitaxy growth.

Moreover, the cavity length is accessible to further microfabrication, regrowth, and surface passivation before the top mirror is deposited. The diode structure before dielectric mirror deposition is ideally suited for the introduction of passive focussing or Fourier optics through microfabrication. Furthermore, the transverse mode structure and polarization can be controlled by judicious placement of gratings or absorbers in the cavity. Magneto-optic and non-linear optical layers can also be introduced into the cavity before the top mirrors are deposited. Finally, we have shown that even continuous contact layers, such as thin Gold or Molybdenum films can be included into the low-intensity region of the optical standing wave in the VCSEL cavities. Finally for etched structures, the total depth to which the microlaser has to be etched is reduced, and for implanted structures, the implantation depth (and the lateral straggle of the ions) is decreased. This is expected to lead to a decrease in the individual laser size and threshold current, which also allows the operation of arrays with a larger number of laser elements.

## REFERENCES

- [1]. K. Iga, S. Koyama, and S. Kinoshita, "Surface emitting semiconductor lasers", IEEE J. Quantum Electronics, vol QE-24, pp1845-1855, 1988.
- [2]. J.L. Jewell, J.P Harbison, A. Scherer, Y.H. Lee, L.T. Florez, "Vertical cavity surface emitting lasers: design, growth, characterization", IEEE J. Quantum Electronics, vol. QE-27, pp1332-1346 1991
- [3]. R.S Geels, S.W. Corzine, L.A. Coldren, InGaAs vertical cavity surface emitting lasers", IEEE J. Quantum Electron., vol QE-27, pp1359-1367, 1991
- [4]. E.F. Schubert, L.W. Tu, R.F. Kopf, G.J. Zydzik, D.G. Deppe, "Low threshold vertical cavity surface emitting lasers with metallic reflectors, Appl. Phys. Lett., 57, p117, 1990
- [5]. H. Wada, D.I. Babic, D.L. Crawford, J.J. Dudley, J.E. Bowers, E.L. Hu, J.L. Merz, M.G. Young, "Low threshold, high temperature pulsed operation of InGaAs/InP vertical cavity surface emitting lasers", IEEE Photon. Tech. Lett., vol 3, pp977-979, 1991
- [6]. T. Baba, Y. Yogo, K. Suzuki, F. Koyama, K. Iga, "Low threshold room temperature pulsed and -31C CW operations of 1.3  $\mu\text{m}$  GaInAsP/InP buried heterostructure surface emitting lasers", Tech. Dig. OFC'93, San Jose, CA, Paper PD28-1, 1993
- [7]. T. Baba, Y. Yogo, K. Suzuki, F. Koyama, K. Iga, "First room temperature cw operation of GaInAsP/InP surface emitting laser", in Tech. Dig., Topical meeting on Quantum Optoelectronics, Palm Springs, CA Paper PD2-2, 1993
- [8]. R.P. Schneider, J.A. Lott, Materials and design challenges for AlGaInP visible vertical cavity surface emitting laser diodes, SPIE Tech. Conf. 2147. Schneider et.al. "Visible (657nm) InGaP/InAlGaP strained quantum well vertical cavity surface emitting laser", Appl. Phys. Lett., 60, 15, pp1830-1832 (1992)
- [9]. A. Scherer, M. Walther, J.P. Harbison, L.T. Florez, "Fabrication of low threshold voltage microlasers", Electron. Lett., vol 28, pp1224-1226 1992
- [10]. A. Scherer, M. Walther, L.M. Schiavone, B.P. Van der Gaag, "Reactive sputter deposition of high reflectivity dielectric mirror stacks", J. Vac. Sci. Technol., (1993)
- [11]. K. Uomi, M. Aoki, T. Tsuchiya, A. Takai, "Dependence of high speed properties on the number of quantum wells in 1.55  $\mu\text{m}$  InGaAs/InGaAsP MQW